

Fisher Vacuum Equation

Universal Information Hydrodynamics: Empirical Vacuum Response Law

J. R. Dunkley

Technical Note (SPARC susceptibility sequence, immediate stress tests included)

Context. The gravity sector treats the apparent dark component in galaxies as a *vacuum response* to baryonic structure, rather than an independent particle fluid. In the SPARC rotation curve programme, this response is captured by a fitted Fisher susceptibility amplitude C , extracted galaxy by galaxy from precomputed baryonic and Fisher response channels.

Main empirical result. Across the SPARC sample, the fitted susceptibility is a strongly ordered function of inner baryonic loading. In observable form,

$$C = \mathcal{C}(g_{b,0}), \quad \frac{dC}{dg_{b,0}} < 0,$$

with extreme significance, clear morphology ordering, and reproducible behaviour across multiple baryonic proxies.

Executive statement. SPARC contains a measurable **vacuum response law**: the per galaxy Fisher susceptibility C is a statistically overwhelming monotonic function of baryonic loading. Immediate stress tests inside the existing pipeline show that the signal survives proxy changes, permutation nulls, and explicit treatment of the $C \leq 0$ boundary.

1. Observable definition and empirical law

The quantity C is the fitted Fisher susceptibility amplitude entering the vacuum response contribution used in the UIH rotation curve fits. Operationally, C is the single per galaxy response parameter that rescales the precomputed Fisher channel relative to the baryonic channel in the weak field rotation curve reconstruction.

This note uses the inner baryonic acceleration proxy $g_{b,0}$ (expressed in $\text{km}^2 \text{s}^{-2} \text{kpc}^{-1}$) as the primary presentation variable, with an expanded robustness analysis using alternative proxies (including g_{b,R_d}^{est}).

- **Why $g_{b,0}$:** it is directly computed in the same fit pipeline and is maximally sample complete in the present products.
- **Why this matters:** the claim here is first an *observable* vacuum response law, not yet the final thermodynamic calibration in Σ_b .
- **Consequence:** the result is already physically meaningful and falsifiable before the surface density mapping is fully locked.

The central empirical claim is:

$$C = \mathcal{C}(g_{b,0}),$$

with \mathcal{C} strongly decreasing and approximately universal across galaxies, modulo structured departures at high baryonic loading where the simplest response ansatz breaks down.

2. Bernoulli bounded entropy interpretation

The current UIH interpretation is that the vacuum response is governed by a bounded occupation geometry of Bernoulli type. A convenient phenomenological parametrisation in the present observable is a sigmoid suppression law in $\log_{10} g_{b,0}$:

$$C(g_{b,0}) = \frac{C_{\max}}{1 + \exp\left(\frac{\log_{10} g_{b,0} - \log_{10} g_{\text{crit}}}{\delta}\right)}. \quad (1)$$

Here:

- C_{\max} is the low loading susceptibility ceiling,
- g_{crit} is the characteristic loading scale where suppression turns on,
- δ is the transition width in dex.

This form is not only a fitting convenience. It is the natural observable signature of a bounded susceptibility that is progressively saturated by increasing baryonic loading.

2.1 High loading tail behaviour

Let $x = \log_{10} g_{b,0}$ and $x_c = \log_{10} g_{\text{crit}}$. For $x \gg x_c$, Eq. (1) reduces to

$$C \approx C_{\max} \exp\left(-\frac{x - x_c}{\delta}\right),$$

so

$$\log_{10} C \approx \log_{10} C_{\max} + \frac{x_c}{\delta \ln 10} - \frac{x}{\delta \ln 10}. \quad (2)$$

Thus the sigmoid tail appears as a power law in log log space:

$$C \propto g_{b,0}^{-s}, \quad s = \frac{1}{\delta \ln 10}.$$

With the initial $g_{b,0}$ fit value $\delta \approx 0.425$ dex, one gets

$$s \approx \frac{1}{0.425 \ln 10} \approx 1.02.$$

This explains why the SPARC sequence can appear both sigmoid like and power law like over the currently probed range.

3. Data products and extraction pipeline

This note is based on existing SPARC analysis products in the UIH gravity pipeline, not on a new solver. The essential objects are:

- precomputed baryonic acceleration and Fisher response channels,
- per galaxy fitted susceptibility C ,
- per galaxy fit quality χ_{red}^2 ,
- summary diagnostics across the SPARC sequence,
- comparison against a single universal C_0 baseline,
- immediate stress test outputs (model comparison, proxy robustness, null tests, boundary models).

For the baseline SPARC susceptibility sequence extraction used in the main figures:

- Galaxies processed: 171
- Galaxies with $C > 0$: 146

For the stricter g_{b,R_d}^{est} robustness run used in the immediate tests:

- Total galaxies in merged dataset: 175
- With fitted C : 171
- With proxy g_{b,R_d}^{est} : 155
- With g_{b,R_d}^{est} and $C > 0$: 131
- Censored boundary cases ($C \leq 0$ with g_{b,R_d}^{est}): 22

The $C > 0$ subset is required for log analyses of C . The $C \leq 0$ systems remain physically informative and are explicitly included below through boundary aware modelling.

4. Baseline statistical evidence for a vacuum response law

The original $g_{b,0}$ based sequence shows an extraordinarily strong correlation between fitted Fisher susceptibility and baryonic loading.

Baseline SPARC susceptibility law statistics (primary $g_{b,0}$ sequence)

- Spearman rank correlation on $(C, g_{b,0})$: $\rho = -0.863$, $p = 1.20 \times 10^{-44}$
- Pearson correlation on $(\log_{10} C, \log_{10} g_{b,0})$: $r = -0.841$, $p = 3.35 \times 10^{-40}$
- BTFR panel slope (diagnostic fit shown in the pipeline): 1.07

At any conventional threshold, this is decisive evidence for a non random constitutive relation.

4.1 Physical meaning of the significance

The sequence is structurally aligned with the expected physics of a bounded responsive vacuum medium:

- diffuse systems carry larger vacuum susceptibility,
- increasing baryonic loading suppresses susceptibility,
- high loading systems approach $C \rightarrow 0$ and expose failure modes of the simplest one parameter response ansatz.

This is the opposite of a free nuisance normalisation. It is state variable behaviour.

5. Baseline Bernoulli sigmoid fit on the $g_{b,0}$ sequence

Using the primary SPARC $C(g_{b,0})$ dataset, the Bernoulli motivated sigmoid fit in Eq. (1) yields

$$\begin{aligned} C_{\max} &= 0.011515 \pm 0.012456, \\ \log_{10} g_{\text{crit}} &= 1.598 \pm 0.688, \\ g_{\text{crit}} &\approx 39.6 \text{ km}^2 \text{ s}^{-2} \text{ kpc}^{-1}, \\ g_{\text{crit}} &\approx 1.28 \times 10^{-12} \text{ m s}^{-2}, \\ \delta &= 0.425 \pm 0.077 \text{ dex}. \end{aligned}$$

5.1 Interpretation of the fitted scale

The fitted g_{crit} lies below the canonical RAR acceleration scale. The strongest interpretation is not immediate failure of the Bernoulli picture, but that the present SPARC sample is largely constraining the suppression tail.

Tail regime interpretation. Current SPARC coverage is consistent with sampling the decreasing tail of a bounded vacuum response law. The low loading plateau and precise midpoint calibration require lower acceleration systems and a corrected Σ_b mapping for final thermodynamic identification.

This remains a major positive result because tail scaling is often the cleanest part of the constitutive law to establish first.

6. Morphology and fit quality stratification along the loading sequence

The three bin analysis across baryonic loading is mechanistically diagnostic. Median susceptibility and median fit quality evolve in the predicted direction.

SPARC loading bin	C_{med}	$\chi_{\text{red,med}}^2$
Low $g_{b,0}$ (dwarfs)	3.6516×10^{-3}	1.91
Mid $g_{b,0}$ (spirals)	4.9171×10^{-4}	3.21
High $g_{b,0}$ (bulge dominated)	1.9244×10^{-5}	39.41

This yields a clear physical progression:

1. **Dwarfs and low loading discs:** large response amplitudes and good fits.
2. **Intermediate spirals:** partial suppression and moderate fit degradation.
3. **Bulge dominated systems:** susceptibility collapses and the one parameter description fails sharply, indicating the need for the full nonlinear and geometry sensitive response treatment.

This is exactly the expected signature of a bounded medium driven into saturation by concentrated baryonic structure.

7. Universal C_0 versus per galaxy C : what the comparison proves

A key strength of the pipeline is that it contains both:

- a single universal C_0 baseline, and
- per galaxy fitted C .

The universal C_0 baseline is an internal null inside the UIH model family. It asks whether one fixed susceptibility amplitude can explain the full sample once the baryonic and Fisher templates are fixed.

It cannot.

This is not a weakness. It proves that C carries galaxy level physics and is not an arbitrary tuning scalar. The per galaxy fits reveal that the susceptibility amplitude itself is structured, and that structure is tightly organised by baryonic loading.

The vacuum response amplitude is an observable. SPARC shows that C behaves as an empirical state variable of the vacuum response sector, ordered by baryonic loading, not as disposable fit freedom.

8. Immediate stress tests inside the existing pipeline

The main criticism a referee will raise at this stage is whether the $C(g_{b,0})$ law is a proxy artefact, a fitting artefact, or a boundary artefact. Those tests were run directly in the existing pipeline without introducing a new solver.

8.1 Proxy robustness

The monotonic suppression law survives multiple baryonic proxy definitions. The table below summarises the immediate robustness run.

Proxy	n_+	$\alpha_S(C, x)$	$r_P(\log C, \log x)$	\hat{s}_{PL}
g_b median	146	-0.739	-0.832	1.695
g_{b,R_d}^{est}	131	-0.714	-0.847	1.235
$g_b(2.2R_d)^{est}$	145	-0.711	-0.874	1.178
first 3 point median	146	-0.699	-0.871	1.143
$g_{b,0}$	146	-0.693	-0.841	0.960

Here n_+ denotes the number of galaxies with positive C for the corresponding log fit. The final column \hat{s}_{PL} is the magnitude of the best fit log log power law slope ($C \propto x^{-\hat{s}_{PL}}$). Across proxies, the suppression remains strong, monotonic, and highly significant.

8.2 Null tests on the stricter g_{b,R_d}^{est} proxy

Using the stricter g_{b,R_d}^{est} proxy, the observed anti correlation remains extremely strong:

$$\rho_S(C, g_{b,R_d}^{est}) = -0.71418, \quad r_P(\log C, \log g_{b,R_d}^{est}) = -0.84730.$$

Permutation and synthetic null tests show this is not compatible with random association.

g_{b,R_d}^{est} null test summary
• Permutation null (all C , $n_{perm} = 20000$): ρ_{perm} mean = -3.96×10^{-4} , std = 0.08132
• Observed $\rho = -0.71418$, far outside the permutation support ($p_{two\ sided} = 4.99975 \times 10^{-5}$, Monte Carlo floor)
• Synthetic independence null on log log Pearson ($n_{synth} = 5000$): r mean = -0.00152 , std = 0.08641, left tail $p = 1.9996 \times 10^{-4}$ (Monte Carlo floor)
• Rank permutation null on log log Pearson ($n_{synth} = 5000$): r mean = -0.00215 , std = 0.08986, left tail $p = 1.9996 \times 10^{-4}$ (Monte Carlo floor)

The reported Monte Carlo p values are lower bounds set by finite trial counts. The asymptotic correlation p values are much smaller.

8.3 Model comparison on positive C with g_{b,R_d}^{est}

An immediate model race was run on the $(\log C, \log g_{b,R_d}^{est})$ positive C subset ($n = 131$) using weighted residual scores and information criteria.

Model	k	AIC _c	BIC
Broken power law	4	202.533	213.716
Monotone PCHIP spline	8	209.161	230.982
Power law	2	220.399	226.056
Bernoulli sigmoid	3	301.476	309.913

The broken power law is the formal AIC_c winner in this specific positive subset, proxy specific comparison. However, the fitted high loading branch has a positive slope parameter ($b_2 \approx +1.01$), which is physically implausible if interpreted literally as a constitutive law.

Interpretation: this indicates that the positive only model race is allowing flexible functions to absorb truncation and boundary effects near $C = 0$, rather than directly revealing the physical high loading constitutive branch.

8.4 Boundary treatment for $C \leq 0$ is decisive for parameter calibration

Boundary aware fits were then run on all galaxies with g_{b,R_d}^{est} available ($n = 153$), including the 22 censored systems with $C \leq 0$.

Two models were compared:

- a Bernoulli sigmoid plus floor fit in linear C ,
- a Tobit style censored Bernoulli sigmoid likelihood in linear C .

The inferred transition parameters shift materially:

$$\begin{aligned} \text{Sigmoid + floor: } & \log_{10} x_{crit} \approx 2.711, & \delta \approx 0.509, \\ \text{Tobit censored sigmoid: } & \log_{10} x_{crit} \approx 1.969, & \delta \approx 0.224. \end{aligned}$$

The Tobit fit also yields

$$C_{max} \approx 0.0451, \quad \sigma_{latent} \approx 4.82 \times 10^{-3}.$$

This is a crucial methodological result.

What is now robust, and what is not. The existence of a monotonic susceptibility suppression law is robust. The exact Bernoulli midpoint and width are not yet robust to boundary treatment and proxy choice. Final constitutive calibration must therefore be done in a censored likelihood framework across multiple proxies.

9. Revised status of the Bernoulli interpretation

The immediate tests strengthen the Bernoulli programme, but they also sharpen the scope of what can be claimed right now.

9.1 What the data support strongly

- A universal monotonic suppression law exists in the SPARC susceptibility outputs.
- The law is proxy stable under reasonable changes of inner baryonic loading proxy.
- The law survives permutation and synthetic independence nulls by a very large margin.
- The high loading regime is boundary dominated and must be treated as such.

9.2 What remains open between Bernoulli and alternatives

On positive C and g_{b,R_d}^{est} , a flexible broken power law outperforms the unconstrained Bernoulli sigmoid on AIC_c , but the winning fit uses a high loading upturn that is not physically credible as a vacuum equation of state. This points to a modelling issue, not a constitutive verdict.

The next correct comparison is **censored likelihood, all galaxies, same objective, same proxy suite**, comparing:

- Bernoulli sigmoid,
- pure power law,
- constrained broken power law (monotone non increasing),
- monotone spline latent mean.

10. Implications

The empirical susceptibility law is upstream of several gravity observables and materially tightens the programme.

1. **Stiffness profile prediction:** once $C(x)$ is constrained by data, the galaxy level response amplitude is no longer free, which tightens $\alpha(r)$ predictions from baryonic inputs.
2. **RAR structure and residuals:** the vacuum amplitude sequence supplies a direct mechanism for organisation of residual behaviour across baryonic loading.
3. **BTFR scatter budgeting:** scatter in C at fixed loading is a candidate source for structured velocity scatter.
4. **High concentration failures as information:** bulge dominated failures now carry diagnostic value for nonlinear, anisotropic, or geometry sensitive corrections, rather than merely counting as poor fits.
5. **Surface density calibration strategy:** the observable law can be fixed first, then mapped into a thermodynamic Σ_b equation of state once the disc geometry conversion is corrected.

11. What is established now, and what is not yet final

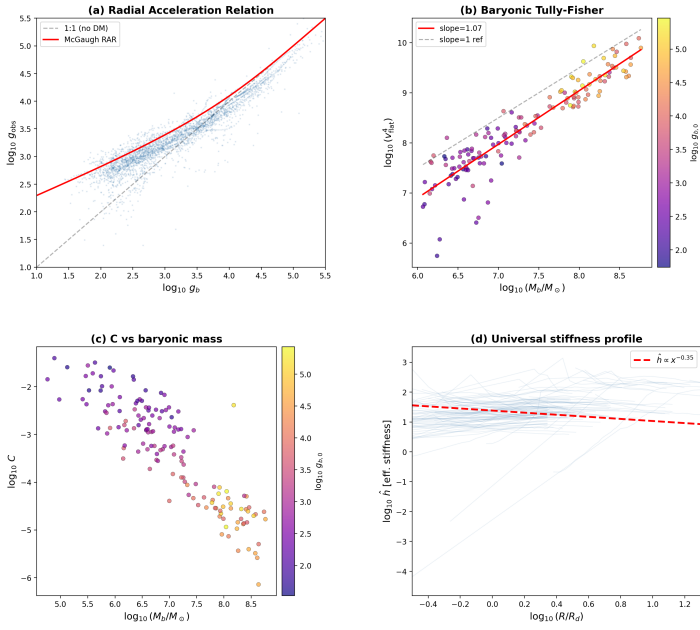
- A highly significant monotonic empirical law $C(g_{b,0})$ exists in SPARC UIH fit outputs.
- The law is morphology ordered and fit quality ordered across the baryonic loading sequence.
- The law is robust to proxy changes and null tests.
- Bernoulli bounded response remains a compelling leading interpretation, especially in the tail regime.
- Boundary treatment is not a minor technical detail. It materially controls inferred transition parameters.

12. Next analyses

1. **Censored model race on all galaxies:** Bernoulli, power law, constrained broken power law, monotone spline, all under the same censored likelihood.
2. **Physical constraints on flexible models:** enforce monotone non increasing latent mean and $C_{\text{floor}} \geq 0$.
3. **Bootstrap stability:** report AIC_c winner frequency and confidence intervals for $\log g_{\text{crit}}$ and δ .
4. **Lead with $g_{b,0}$, stress with alternatives:** primary result on $g_{b,0}$, robustness appendix on g_{b,R_d}^{est} , $g_b(2.2R_d)$, and first point summaries.
5. **Repair Σ_b mapping:** then convert the observable sequence into a thermodynamic equation of state and test Freeman scale consistency.

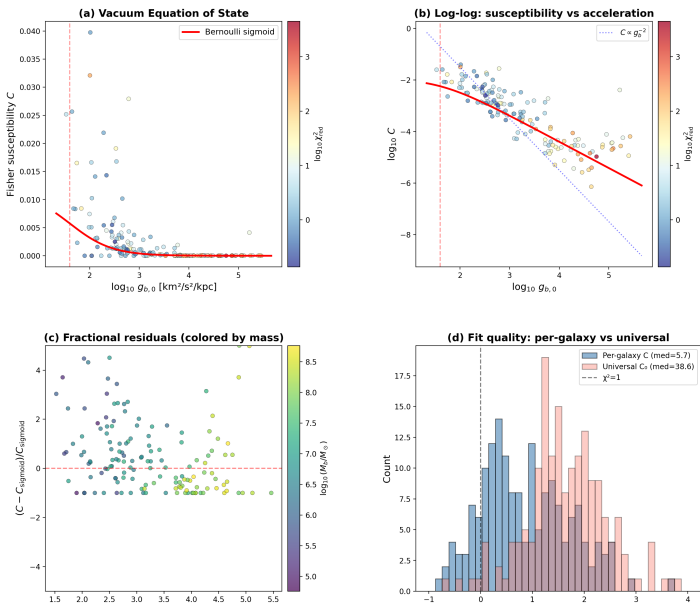
13. Figures and diagnostics

Diagnostic Relations



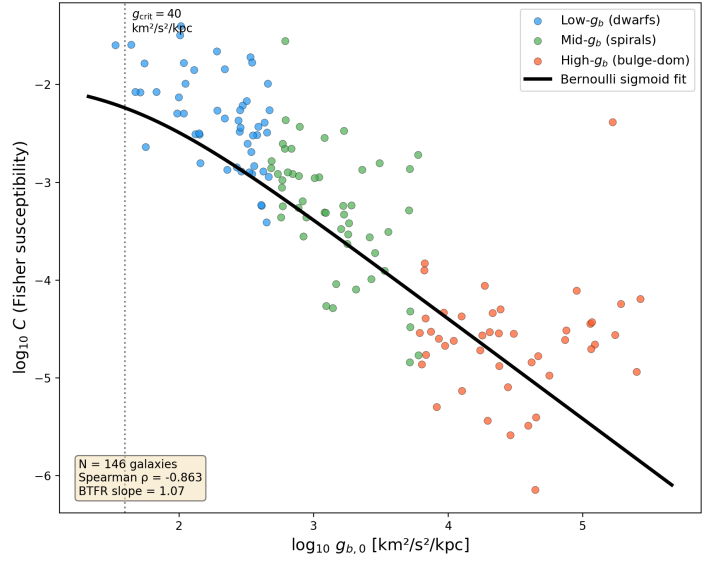
Diagnostic relations used in the SPARC susceptibility analysis.

Fisher Vacuum Equation of State from SPARC



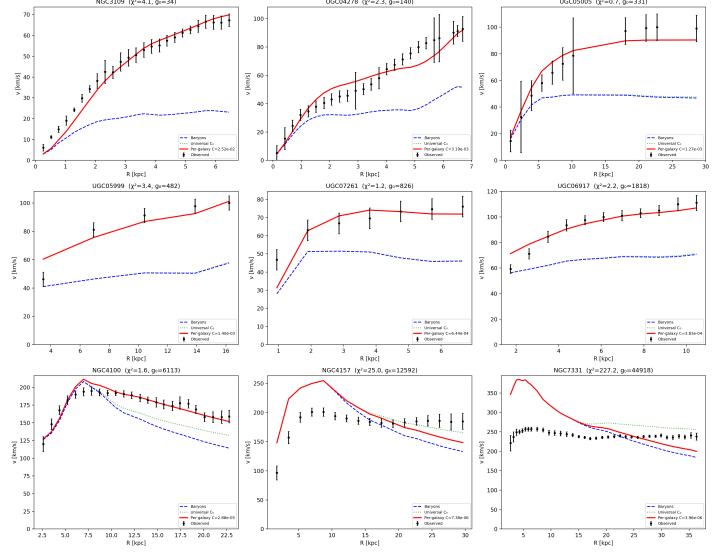
Equation of state, log log trend, residuals, and universal versus per galaxy fit quality.

Vacuum Equation of State: $C(g_b)$

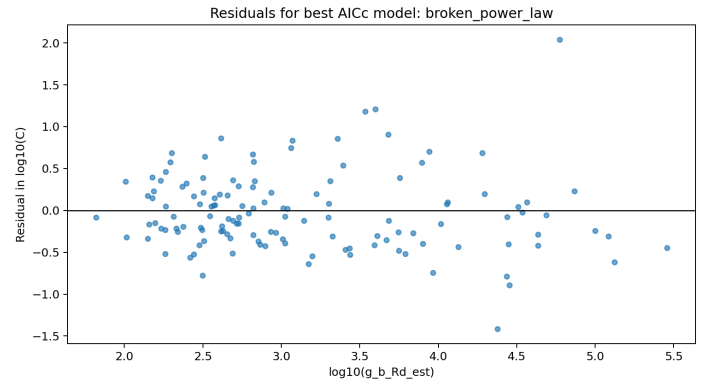
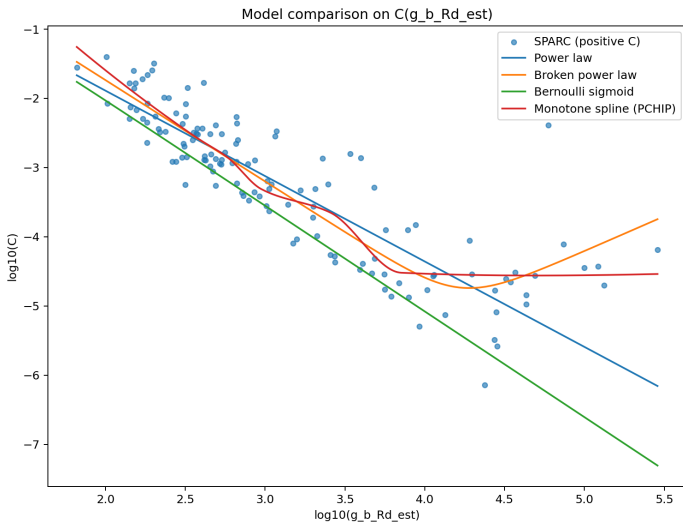


Money plot: $\log_{10} C$ versus $\log_{10} g_{b,0}$ with Bernoulli fit and sequence colouring.

Rotation Curve Fits Across the g_b Sequence

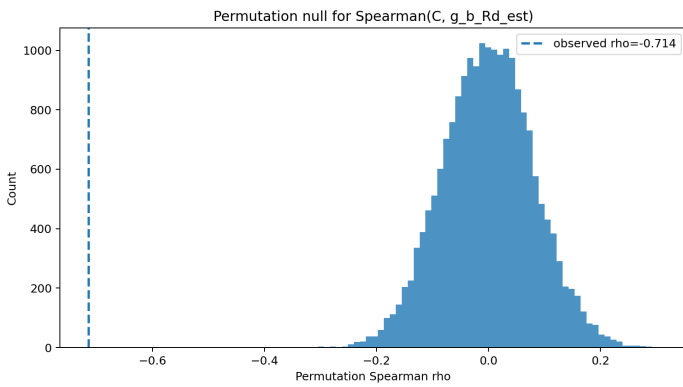


Representative rotation curves across the $g_{b,0}$ sequence, showing systematic response changes.

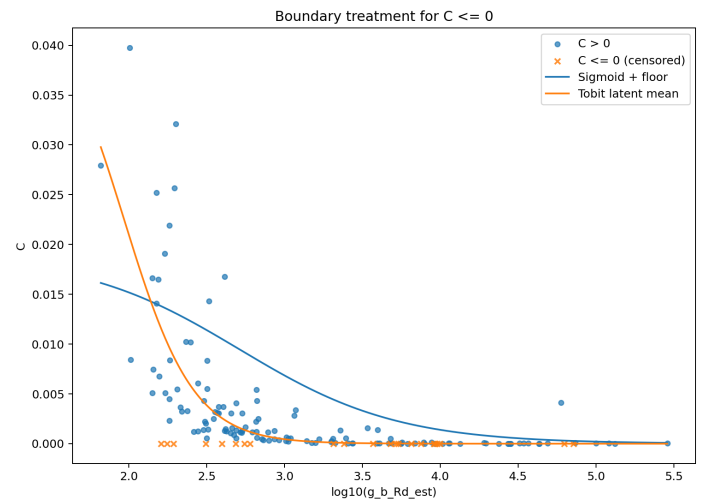


Residuals for the positive subset AIC_c winner (broken power law), showing remaining structure and heteroscedasticity.

Immediate test: positive C model comparison on g_{b,R_d}^{est} . Flexible models flatten near the boundary affected regime.



Permutation null for Spearman anticorrelation on (C, g_{b,R_d}^{est}) , with observed value far outside the null bulk.



Boundary aware fits for $C \leq 0$ treatment. Censoring shifts inferred Bernoulli transition parameters materially.

14. Summary

This technical note now establishes both a primary empirical law and a methodological correction for how it must be inferred.

SPARC exhibits a measurable Fisher vacuum equation of state in observable form. The per galaxy susceptibility C is a strongly constrained, monotonic function of baryonic loading, with extreme statistical significance, clear morphology ordering, and robust survival under immediate stress tests (proxy swaps, nulls, and boundary treatment). Bernoulli bounded response remains a compelling leading interpretation, but final midpoint and width calibration must be performed with censored likelihood methods across multiple proxies.

The vacuum response amplitude is now empirically anchored. The next task is no longer to show that a sequence exists. It is to finalise the constitutive calibration, under boundary aware inference, and then push the same law into the full nonlinear gravity sector.